Journal of the Serbian Chemical Society
JSCS-info@shd.org.rs • www.shd.org.rs/JSCS
J. Serb. Chem. Soc. *84* (11) 1305–1318 (2019)
JSCS–5265
UDC 546.824–31:549.753.11–36+539.61+542.8
Original scientific paper

Relationship between the properties of an interlayer formed by *in situ* Ti anodization and anaphoretically deposited hydroxyapatite

MARIJANA R. PANTOVIĆ PAVLOVIĆ[1,2#], MIROSLAV M. PAVLOVIĆ[1#], SANJA ERAKOVIĆ[1#], TANJA BARUDŽIJA[3], JASMINA S. STEVANOVIĆ[1,2*], NENAD IGNJATOVIĆ[4] and VLADIMIR V. PANIĆ[1,2,5#]

[1]Institute of Chemistry, Technology and Metallurgy, University of Belgrade, Njegoševa 12, Belgrade, Serbia, [2]Centre of Excellence in Environmental Chemistry and Engineering – ICTM, University of Belgrade, Njegoševa 12, Belgrade, Serbia, [3]Vinča Institute of Nuclear Sciences, University of Belgrade, 12–14 Mike Petrovića Street, Belgrade, Serbia, [4]Institute of Technical Science of the Serbian Academy of Sciences and Arts, Knez Mihailova 35, Belgrade, Serbia and [5]State University of Novi Pazar, Department of Chemical-Technological Sciences, Novi Pazar, Serbia

(Received 30 July, revised 23 September, accepted 24 September 2019)

Abstract: The optimization of the anodization process of Ti substrate for *in situ* synthesis of hydroxyapatite/titanium oxide composite coatings on titanium substrate was accomplished. The anodization was performed under 30, 60 and 90 V cell voltage, and the morphology of treated surface, as well as linear and surface roughness, were analysed by field emission-scanning electron microscopy, atomic force microscopy and roughness tester. It was shown by linear and surface roughness analyses that titanium anodized under 60 V has the highest roughness, whereas at 90 V the flattening of the surface occurs. As the highest surface roughness results emerged at 60 V, the novel process of composite anHAp/TiO_2 coating synthesis, which comprises simultaneous processes of TiO_2 formation and HAp deposition, as well as HAp impregnation within TiO_2 surface layer, was performed at this voltage. Ti substrate surface was completely covered by composite coating, with no visible cracks. The adhesion quantified according to ASTM D3359-02 standard is considerably improved with respect to the coatings obtained by cathaphoretic processes, with no need of subsequent sintering.

Keywords: titanium anodization; roughness; *in situ* anaphoretic deposition; hydroxyapatite coating; adhesion; titanium oxide.

* Corresponding author. E-mail: j.stevanovic@ihtm.bg.ac.rs
# Serbian Chemical Society member.
https://doi.org/10.2298/JSC190730105P

INTRODUCTION

Titanium and its alloys are widely used in medical devices, orthopedic implants, dental implants, and device components of aerospace industries. It is attractive for its low weight, fatigue resistance, corrosion resistance, having superior room and elevated temperature mechanical properties.[1–4] As one of the valve metals (others being Al, Ta, Nb, V, Hf and W), titanium is protected by a thin oxide layer which spontaneously forms on its surface when exposed to air or other oxygen-containing environments. This 2- to 5-nm thick oxide passive layer is responsible for the corrosion resistance of titanium and its alloys.[5] Due to its passivating oxide layer, titanium is biocompatible and used as implant material in various medical devices. However, the native TiO_2 layer is not bioactive enough and it lacks osseointegration to form a direct bonding to the bone. This can lead to long term failure after implantation.[5] Improvement of the surface properties of titanium-based implants (*e.g.*, topography, chemistry and surface energy) include surface modification techniques such as sand-blasting, acid etching, plasma spraying, *etc.*[5–10]

Anodization is another widely used method to improve bioactivity by formation of protective oxide films on titanium and its alloys.[3,11–13] The advantages of this technique include ease of production, strong adhesion between the oxide layer and the substrate and superior control of the surface morphology.[14–16] The anodization process consists of applying an anodic current to the Ti and Ti alloys substrate in different electrolyte solutions. The parameters of anodization, such as electrolyte type, temperature, anodic current density and anodization time, significantly affect the properties and morphologies of the anodic oxide films.[17–19]

On the other hand, neither mechanical nor chemical methods have the ability to produce controlled surface topographies, since these methods have the potential to form surface residuals. Alternative methods to modify titanium surfaces are required. One of the most promising attempts to further improve bone-bonding involves coating titanium-based implants with hydroxyapatite (HAp) or other calcium phosphates.[5] HAp is the main mineral in bones with the Ca/P mole ratio of 1.67 in stoichiometric hydroxyapatite ($Ca_{10}(PO_4)_6(OH)_2$).[4] The HAp-coated titanium was shown to have excellent corrosion resistance and good biocompatibility.[20] HAp is of porous structure and sufficient bioactivity for its partial resorption leading to successful replacement of natural bone cells. It is widely used in medical applications, including tissue engineering, drug delivery and bone tissue repair, owing to ability to create strong chemical bonds with bones.[4,21]

The main problem in altering titanium surface by ceramic coatings is large difference in properties of the hydroxyapatite and titanium substrate. The coating adhesion to the substrate remains a major problem due to different mechanical properties.[4] Literature review showed that most of the papers did not address adhesion problem.[22–26] Poor coating adhesion appeared in the form of delamin-

ation, poor mechanical properties, poor connections between ceramics and metals and long-term failures due to weak adhesion to the metal substrate and dissolution once they have been implanted.[4,5] Solutions to this problem were partially found in the surface modification methods of the substrate, such as anodization, sandblasting, electrophoretic deposition of HAp coatings or chemical treatment of the surface to improve adhesion.[27,28] With electrodeposition, HAp coatings of complex structures can be obtained, with easily controlled thickness at low temperature.[20,28]

In order to address known problems associated with controlled surface topography, morphology and adhesion, novel *in situ* synthesis of HAp/TiO_2 composite coating on titanium substrates, *via* electrophoretic deposition (EPD) of HAp and simultaneous anodization of Ti is reported. the applied synthesis methodology is expected to strengthen the biocompatible composite coating with no need of subsequent sintering.

EXPERIMENTAL

Titanium plates (Aldrich, 99.7 % purity) with a dimension of 20 mm×10 mm×0.89 mm were used as the substrates. Prior to anodization, samples were abraded with silicon carbide (SiC) paper of successive grades from 600 to 2000 grit and further mechanically polished to mirror finish with alumina pastes of 1, 0.3 and 0.05 μm. All samples were then ultrasonically cleaned in ethanol solution and rinsed in deionized water.

Anodization was carried out in an electrolytic cell with a magnetic stirring at 25 ºC. The prepared sample was used as anode, and a 1Cr18Ni9Ti stainless steel plate as cathode. The electrolyte was an aqueous solution consisting of 50 vol.% 0.1 M sodium hydroxide (NaOH) and 50 vol.% of absolute ethanol, which were prepared from analytical grade chemicals (Sigma–Aldrich) and deionized water. A Hewlett Packard HP6024A potentiostat/galvanostat was served as a power supply. The cathodes faced both sides of the anode with the distance between the anode and the cathodes of 10 mm. The anodizing voltages applied were 30, 60 and 90 V. The samples were anodized until 1.13 C of electric charge was consumed by the anode. The reason for choosing to conduct Ti substrate anodization process up until 1.13 C of electric charge was spent by the anode is to control both the speed and time of anodization, After anodization, the titanium specimens were rinsed with deionized water and cleaned in an ultrasonic bath. Afterwards, the coatings were dried at 80 °C for 30 min.

The morphology and roughness of the anodized samples were examined by FE-SEM (Tescan Mira 3 XMU FEG-SEM) and AFM (Nanoscope III AFM multi-mode scanning probe microscope, produced by Digital Instruments).

A chemical precipitation method was used to prepare HAp powder by the reaction of calcium oxide (obtained by calcination of $CaCO_3$ for 5 h at 1000 °C in air) and phosphoric acid. A stoichiometric amount of the calcium oxide was stirred in distilled water for 10 min and phosphoric acid was added dropwise to the suspension in order to obtain hydroxyapatite powder, $Ca_{10}(PO_4)_6(OH)_2$. When the necessary quantity of phosphoric acid was introduced, the pH reached the value of 7.4−7.6. The obtained suspension was heated to 94±1 °C for 30 min and stirred for another half an hour. Upon sedimentation, the upper clear solution layer was decanted. The suspension was spray-dried at 120±5 °C into granulated powder.[29]

For anaphoretic deposition, the HAp suspension was prepared from 1.0028 g of HAp powder and 100 cm^3 of solution containing 50 vol. % of absolute ethanol and 50 vol. % of 10 % NaOH water solution (pH 10). Subsequently, suspension was ultrasonicated for 15 min to reach homogeneous and stable state. The titanium plates (dimensions: 20 mm×10 mm×0.89 mm, for surface analysis, Aldrich, 99.7 % purity) were used as substrates for anaphoretic deposition of HAp coatings. As for anodization, Ti plates were mechanically pretreated before deposition. Metal plates were polished with different grades sandpaper, followed by wet polishing with 0.3 and 0.05 μm alumina and finally cleaned in ethanol for 15 min in an ultrasonic bath.

The electrochemical cell was filled with HAp/NaOH suspension and purged with N_2 for 30 min. A Hewlett Packard HP6024A potentiostat/galvanostat was used as power supply. Prior to anaphoretic depositions, the HAp suspension was ultrasonically treated for 30 min to obtain a homogeneous particle distribution and the suspension was stirred for 2 h by magnetic stirrer prior and continuously during anaphoretic deposition. The HAp/TiO_2 (anHAp/TiO_2) composite coatings on Ti were obtained at the constant voltage of 60 V for a deposition time of 45 s, at 25 °C. AnHAp/TiO_2 coatings were air dried at room temperature.

The morphology and roughness of the obtained anHAp/TiO_2 coating was examined by SEM and AFM. Linear roughness of both anodized Ti as well as composite anHAp/TiO_2 coating was measured using portable roughness tester TR-200 (Innovatest, Maastricht, The Netherlands). Adhesion of *in situ*-synthetized composite anHAp/TiO_2 coating to the titanium substrate was measured according to ASTM D 3359-02: Standard Test Methods for Measuring Adhesion by Tape; cross-cut tape test (B).

RESULTS AND DISCUSSION

Optimization of deposition parameters – anodization of titanium

The current applied to anode *vs.* time of anodization in first 50 s of the anodization is plotted in Fig. 1. There is well-resolved current peak in first few

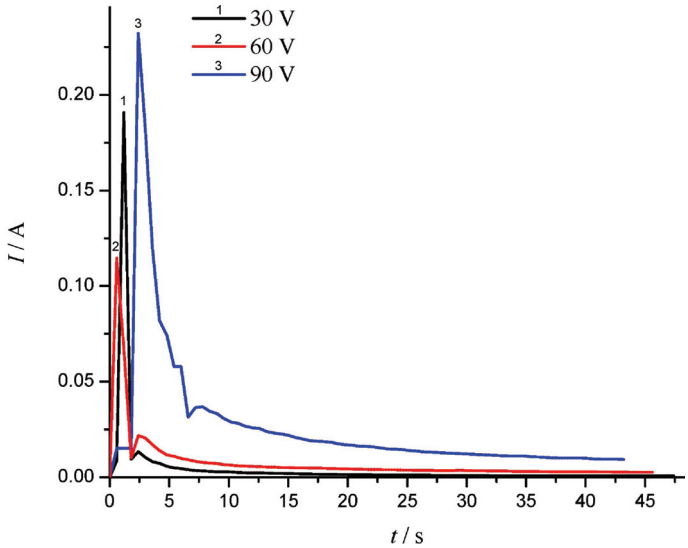

Fig. 1. Current transient for the first 50 s of anodization process. Anodized Ti area is 2 cm^2.

seconds of the anodization process, when the majority of the anodization process take place and when the most of the electric charge is spent. Once the non-conductive oxide titanium layer is formed on the substrate surface, the current drops sharply, and exponentially decays throughout the experiment. The total electric charge applied to the anode can be calculated by integrating *I vs. t* curves. The electric charge of 1.13 C required 5235 s at 30 V, 1785 s at 60 V and only 49 s at 90 V of anodization.

Table I shows the time distribution required for different electric charges to pass through the anode at various anodization voltages.

TABLE I. Time distribution for anode (in s) to receive certain electric charge during anodization process for different voltages

Electric charge, C	Anodization voltage, V		
	30	60	90
0.90	4211	1039	30
1.00	4747	1403	39
1.13	5235	1785	49

Fig. 2 shows the appearance of untreated and the anodized titanium substrates at different anodization voltages, namely 30, 60 and 90 V. The prepared Ti substrate without anodization appears gray with mirror-like metallic shine (Fig. 2a). However, the substrate becomes turquoise by anodization at 30 V (Fig. 2b). This change in color indicates that a new oxide layer is formed on the surface. By increasing the applied voltage to 60 V, then keeping the electric charge constant (*i.e.*, 1.13 C), the surface of anodized layer becomes orange with inputs of purple spots on the surface of orange oxide layer (Fig. 2c). This color change indicates that new oxide layer is formed, which took 1785 s for the Ti substrate to spent 1.13 C (Table I). As the anodization voltage is further increased to 90 V, the titanium surface appears navy blue, with edges still being purple (Fig. 2d). It can be concluded that the oxide layer color for the constant electric charge of anodization changes from turquoise to yellow, orange, purple and finally navy

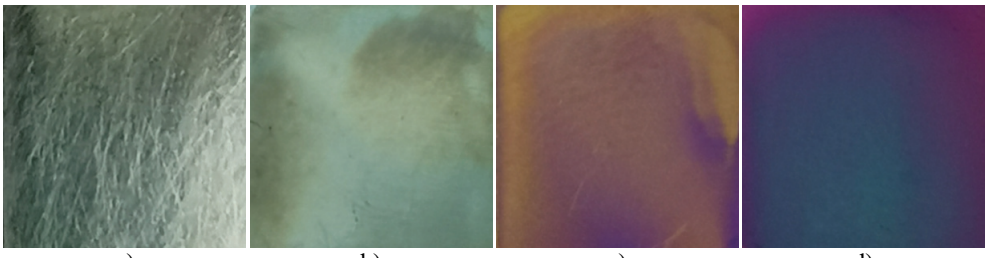

a) b) c) d)

Fig. 2. Optical images of titanium substrate, a) no anodization; anodization at: b) 30, c) 60 and d) 90 V.

blue, depending on applied voltage.[3,30] The absence of uniform color can be explained by uneven primary current density distribution – current densities are not the same at the center of substrate and towards the edges.[31] The electric charge received by the substrate is not the same at every point of the substrate.

Fig. 3 shows surface morphology of the titanium substrate and anodic oxide films obtained by applying different voltages during anodization process, keeping the applied electric charge on anode constant. Before anodization, the surface of polished sample was smooth and homogeneous (Fig. 3a). By increasing the anodization voltage, the increase in surface roughness can be observed for 30 and 60 V (Fig. 3b and c), whereas some flattening of the surface happens (Fig. 3d), although the roughness appears to be higher at 90 V than for 60 V. This is confirmed by linear and surface roughness analyses (Figs. 4 and 5 and Tables II and III).

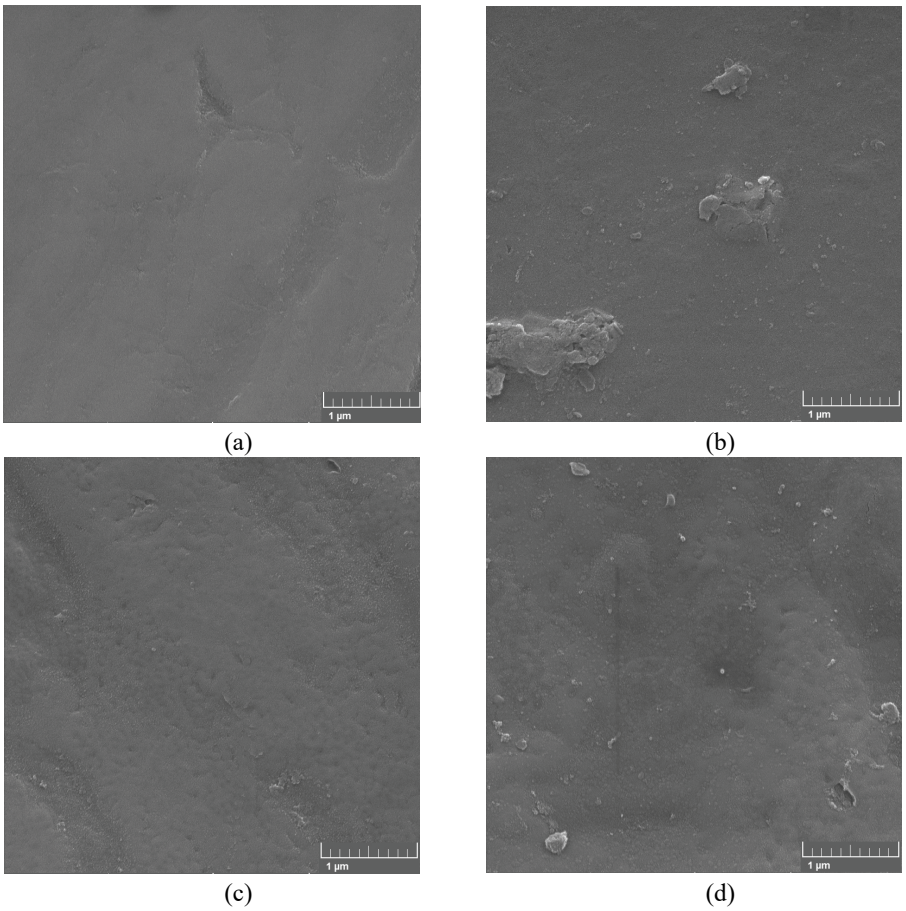

(a) (b) (c) (d)

Fig. 3. FE-SEM images showing surface morphology of: a) untreated Ti substrate and the anodic oxide films on titanium obtained at: b) 30, c) 60 and d) 90 V.

Anodization at 30 V leads to formation of compact oxide layer on the surface of Ti substrate (Fig. 3b), with some small bumps corresponding to secondary oxide particles. These can be defined as secondary oxide particles, since the difference between them and primary oxide layer is evident. Conducting anodization process at 60 V leads to complete coverage of the titanium surface by secondary oxide layer (Fig. 3c), and the substrate has increased roughness regarding untreated Ti plate and Ti plate anodized at 30 V. On the other hand, anodization at 90 V changes the substrate surface roughness further (Fig. 3d), in the sense that surface becomes even smoother. The morphological features change in sense that the surface peaks broaden and the valleys, *i.e.*, vacancies, fill-up, causing the surface to be smoother. These processes lowered the root-mean-square roughness (*RMS*), Table II and Fig. 4.

TABLE II. The results of measurements of different roughness parameters; *Ra* – arithmetic mean of the absolute values of profile deviation from mean within sampling length; *Rq* = *RMS* – the square root of the arithmetic mean of the squares of profile deviation from mean within sampling length; *Ry* – the sum of height of the highest profile peak from the mean line and depth of the deepest profile valley from the mean line within sampling length; *Sm* – the mean spacing between profile peaks at the mean line within sampling length

Sample	*Ra* / μm	*Rq* / μm	*Ry* / μm	*Sm* / mm
Pure Ti substrate	0.047	0.062	0.374	0.0328
Anodized Ti 30 V	0.140	0.177	0.778	0.0500
Anodized Ti 60 V	0.207	0.254	1.131	0.0378
Anodized Ti 90 V	0.168	0.213	0.640	0.0245

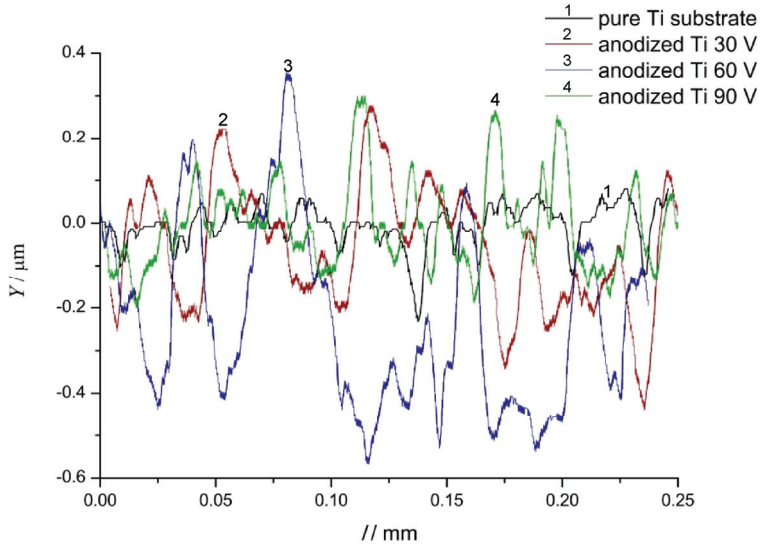

Fig. 4. Linear roughness profiles of untreated and Ti substrates anodized at different voltages. *Y* is profile deviation and *l* is measuring length.

It can be seen from Fig. 4 that the linear roughness increases as the applied voltage increases up to 60 V, and then it decreases when Ti is anodized at 90 V. Non-anodized Ti substrate has low values of *Ra*, *Rq* (*RMS*) and *Ry*. Upon anodization at 30 V, *Ra* and *Rq* drastically increase, and the profile becomes coarser. On the primal oxide layer, second oxide layer in the form of islands start to appear on the surface, which can be seen from increased *Sm* value (the mean spacing between profile peaks at the mean line within sampling length). This measurement is in accordance with observations from Fig. 3b. At 60 V, the formation of the secondary oxide layer is the most visible. *Ra* and *Rq* values almost double regarding anodization at 30 V and the peaks grow higher, while the valleys dig deeper (*Ry*). The *Sm* value decreases, which is the indicator of complete coverage of the titanium surface by secondary oxide layer. At 90 V of anodization, specific changes take place. Although the *Ra* and *Rq* values decrease, which indicates some flattening of the surface, *Ry* value suggests that the valleys started to fill with oxide layer and accordingly the peaks got broadened, Fig. 4. Accordingly, the *Sm* value at 90 V is the lowest among the samples, which leads to the conclusion that the surface is wavier, and that oxide layer grows uniformly.

Further insight into anodization features is analyzed by AFM. Fig. 5 shows three-dimensional AFM images of untreated titanium substrate and those of ano-

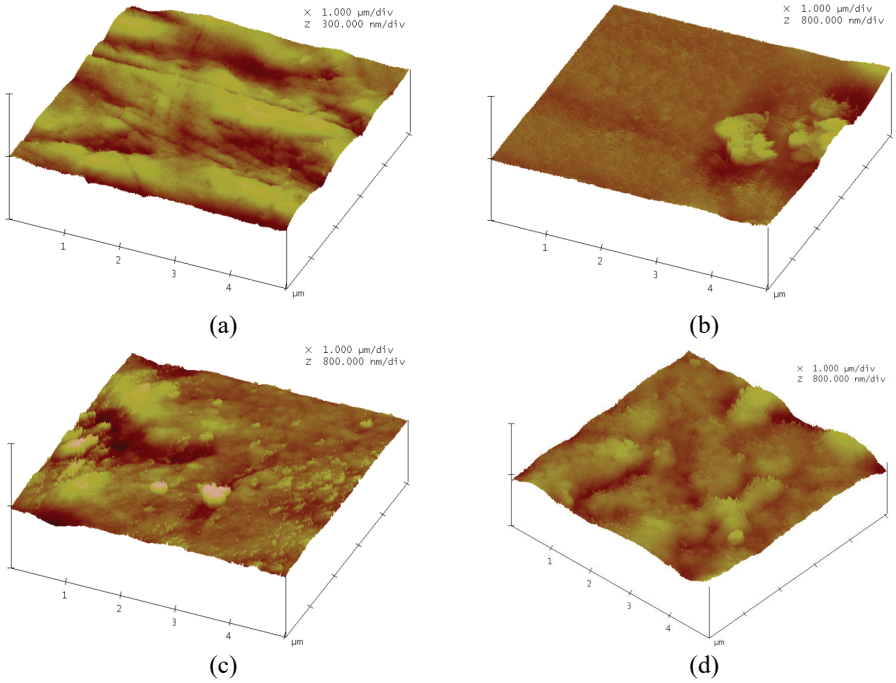

Fig. 5. Three-dimensional AFM images of: a) untreated Ti substrate and anodic oxide films on titanium obtained at: b) 30, c) 60 and d) 90 V.

dized ones at 30, 60 and 90 V. The microscopy data was processed with NanoScope Analysis software and information regarding surface roughness was obtained. Table III shows the values of root-mean-square roughness (*Rq* or *RMS*) obtained from the AFM image of recorded area (5×5 μm^2). Untreated Ti plate (Fig. 5a) has smooth surface. It should be taken into account the height of the recorded profiles. For untreated Ti it is 300 nm div^{-1}, and for all the other samples (Fig. 5b–d) it is 800 nm div^{-1}. For anodization at 30 V (Fig. 5b), the anodic oxide film is compact with some small bumps of secondary oxide layer, and the surface roughness is relatively low. At 60 V (Fig. 5c) the surface is considerably rougher, since the whole surface is covered with secondary oxide layer. The appearance of non-uniform surface in the oxide film caused an increase in surface roughness. The secondary oxide layer continued to grow up at 90 V (Fig. 5d), but once the planar growth of oxide layer occurs, the surface roughness decreases. This can be attributed to a smoothening of secondary oxide layer.

TABLE III. *Rq* (*RMS*) value obtained from AFM measurements for different samples

Sample	untreated Ti	anTi 30 V	anTi 60 V	anTi 90 V
Rq / nm	9.80	13.76	39.43	31.95

In-situ *synthesis of hydroxyapatite/titanium oxide composite coatings on titanium substrate*

The voltage of 60 V was chosen for *in-situ* synthesis of hydroxyapatite/titanium oxide composite coatings on titanium substrate since the Ti surface anodization at this voltage produced the roughest substrate surface.

Fig. 6 shows FE-SEM image of composite anHAp/TiO_2 coating obtained by this novel anaphoretic method.

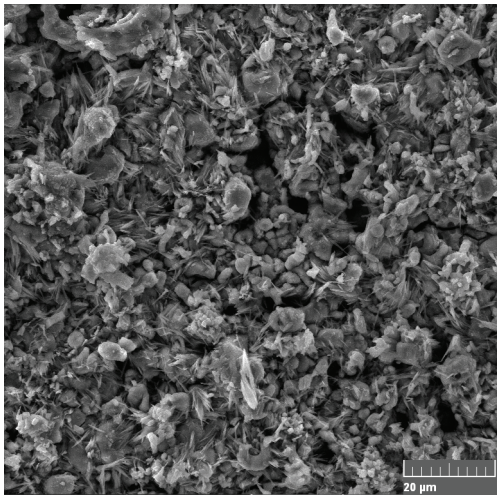

Fig. 6. FE-SEM microphotograph of anHAp/TiO_2 composite coating obtained by *in-situ* synthesis at 60 V.

It can be seen from the Fig. 6 that the coverage of the Ti substrate is complete. There are no visible cracks of the ceramic coating, leading to the conclusion that simultaneous processes of TiO_2 formation, HAp deposition and HAp incorporation into TiO_2 matrix occurs, which is well explained by Pantović Pavlović *et al.*[4] Granular HAp shapes can be observed in Fig. 6. Granular particles are obtained by agglomerating growth of needle-like particles originating from starting HAp powder.[4]

Fig. 7 shows the results of linear roughness analysis of composite anHAp/TiO_2 coating performed in the same manner as for anodization linear roughness measurements.

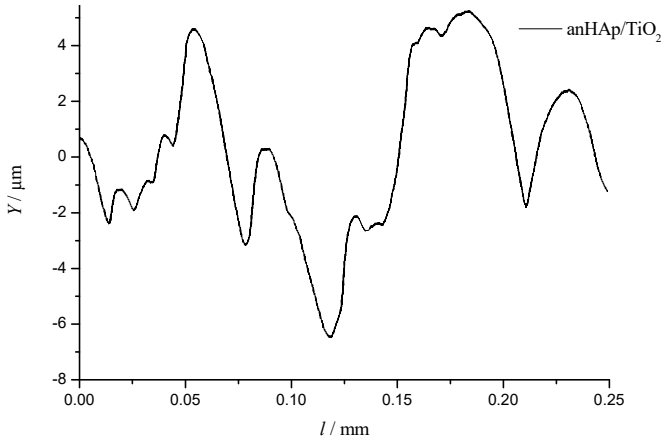

Fig. 7. Linear roughness profile of composite anHAp/TiO_2 coating obtained at 60 V. *Y* is profile deviation, and *l* is measuring length.

Linear roughness measurements confirm the observations about the morphology of composite anHAp/TiO_2 coating on Ti substrate, *i.e.*, the surface is order of magnitude rougher than the surface of anodized Ti. Since rough surface is required for good implant, this coating is good prerequisite for medical implants. It can probably show preferred osseointegration in forming direct bonding with a bone. All of the roughness values, namely *Ra*, *Rq*, *Ry* and *Sm* are much greater than for anodized Ti. These values are: $Ra = 1.712$ µm, $Rq = 2.141$ µm, $Ry = 8.581$ µm and $Sm = 0.0735$ mm. It can be seen from these values that HAp particles are agglomerated, and *Sm* value is good indicator of the size of these agglomerates.

Fig. 8 shows three-dimensional AFM image of composite anHAp/TiO_2 coating obtained by novel *in-situ* synthesis method. As for the anodized samples, the microscopy data was processed with NanoScope Analysis software and information regarding surface roughness was obtained. Recorded area was the same as

for anodized samples (5×5 μm^2). The height division of the recorded profile is 1500 nm div^{-1}.

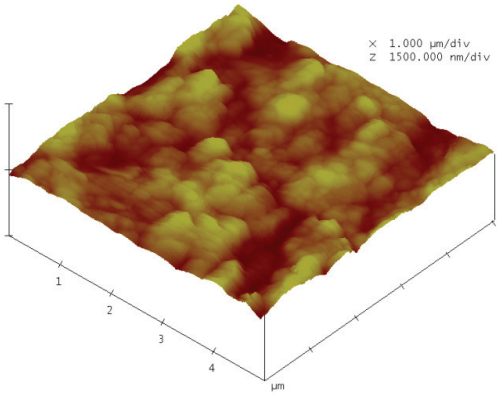

Fig. 8. Three-dimensional AFM images of composite anHAp/TiO_2 coating obtained at 60 V.

The *Rq* value of the surface was 74.437 nm. It can be seen that the surface has much greater *Rq* value than anodized Ti surfaces, which is already shown by linear roughness measurements.

Since the adhesion is the most important feature of HAp coatings on Ti substrate for the application of this composite material in medical science, the adhesion test was performed. Adhesion strength was quantified by adhesion test according to ASTM D 3359-02: Standard Test Methods for Measuring Adhesion by Tape; cross-cut tape test (B). The optical image of the coating after performing adhesion testing is shown in Fig. 9.

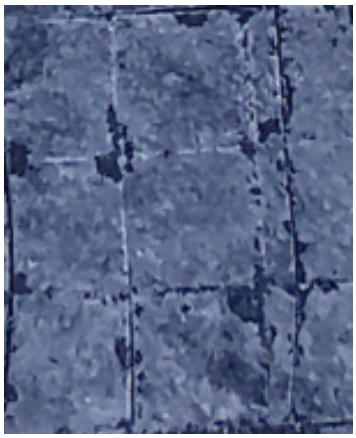

Fig. 9. Optical image of composite anHAp/TiO_2 coating obtained at 60 V after performing adhesion testing according to ASTM D 3359-02.

By evaluating, quantifying and classifying the adhesion of composite anHAp/TiO_2 coating according to ASTM D3359-02 standard, it can be concluded that adhesion is level 4, where 5 is the best adhesion (no delamination and

no flaking) and 0 is the worst adhesion (more than 65 % of the coating delaminated). Comparing to standard cathaphoretic method of HAp deposition, which has level 0 adhesion before sintering and level 1 or 2 (depending of surface pretreatment) after sintering, this novel method is a huge improvement, having in mind that the sintering was applied.

CONCLUSION

Anodization of Ti substrate was performed under 30, 60 and 90 V in order to determine the best conditions for subsequent *in-situ* synthesis of hydroxyapatite/titanium oxide composite coatings on titanium substrate. The linear and surface roughness analyses have shown that titanium anodized at 60 V has the highest roughness, and that at 90 V flattening of the surface occurs; the valleys start to fill with oxide layer and the peaks broaden, pointing out that anodization of Ti at 90 V makes surface less coarse. Novel process of composite anHAp/TiO_2 coating synthesis comprises simultaneous processes of TiO_2 formation and HAp, as well as HAp incorporation into TiO_2 matrix. Ti substrate surface is completely covered by HAp/TiO_2 composite coating. There are no visible cracks. The surface is one order of magnitude rougher compared to anodized Ti obtained at the same anodization voltage. The adhesion, quantified by ASTM D3359-02 standard, is considerably improved as compared to the same coatings obtained by cathaphoretic processes, even without sintering of the coatings. This novel *in-situ* process of HAp coating deposition can provide excellent material for medical implant application.

Acknowledgements. This work was financially supported by Ministry of Education, Science and Technological Development of the Republic of Serbia under the research project ON172060.

ИЗВОД

СВОЈСТВА МЕЂУСЛОЈА НАСТАЛОГ Ti АНОДИЗАЦИЈОМ И *in-situ* АНАФОРЕТСКИ ИСТАЛОЖЕНОГ ХИДРОКСИАПАТИТА

МАРИЈАНА Р. ПАНТОВИЋ ПАВЛОВИЋ[1,2], МИРОСЛАВ М. ПАВЛОВИЋ[1], САЊА ЕРАКОВИЋ[1], ТАЊА БАРУЦИЈА[3], ЈАСМИНА С. СТЕВАНОВИЋ[1,2], НЕНАД ИГЊАТОВИЋ[4] и ВЛАДИМИР В. ПАНИЋ[1,2,5]

[1]Институт за хемију, технологију и металургију, Универзитет у Београду, Његошева 12, Београд, [2]Центар изузетних вредности за хемију и инжењеринг животне средине – ИХТМ, Универзитет у Београду, Његошева 12, Београд, [3]Институт за нуклеарне науке Винча, Универзитет у Београду, Мике Петровића Аласа 12–14, Београд, [4]Институт техничких наука Српске академије наука и уметности, Кнез Михаилова 35, Београд и [5]Државни универзитет у Новом Пазару, Одсек за хемијско–технолошке науке, Нови Пазар

Процесом анодизације титанског супстрата у циљу накнадне *in-situ* анафортеске синтезе композитних превлака хидроксиапатит/титан-оксид формиран је оксидни слој на титанској подлози. Анодизација је рађена на напонима на ћелији од 30, 60 и 90 V, а испитивани су морфологија третиране површине, као и линеарна и површинска храпавост, помоћу FE-SEM, AFM и тестера храпавости, редом. Анализом линеарне и површинске храпавости показано је да титан анодизован на 60 V има највећу храпавост, док при анодизацији на 90 V долази до равнања површине. Како је највећа храпавост површине добијена при анодизацији на 60 V, нови процес композитне синтезе anHAp/TiO_2

превлака, који се састоји од истовремених процеса формирања TiO_2, анафоретског таложења HAp и уградње HAp у TiO_2 матрицу, изведен је при овом напону. Површина титанске подлоге је била потпуно покривена композитном превлаком, без видљивих пукотина, док је адхезија, квантификована ASTM D3359-02 стандардом, знатно побољшана у поређењу са истим превлакама добијеним катафоретским процесима, чак и без накнадног синтеровања превлаке.

(Примљено 30. јула, ревидирано 23. септембра, прихваћено 24. септембра 2019)

REFERENCES

1. S. D. Kahar, A. Macwan, R. Oza, V. Oza, S. Shah, *J. Eng. Res. Appl.* **3** (2013) 441.
2. Z. M. Yan, T. W. Guo, H. B. Pan, J. J. Yu, *Mater. Trans.* **43** (2005) 3142 (https://doi.org/10.2320/matertrans.43.3142)
3. L. Wu, J. Liu, M. Yu, S. Li, H. Liang, M. Zhu, *Int. J. Electrochem. Sci.* **9** (2014) 5012.
4. M. R. Pantović Pavlović, S. G. Eraković, M. M. Pavlović, J. S. Stevanović, V. V. Panić, N. L. Ignjatović, *Surf. Coatings Technol.* **358** (2019) 688 (https://doi.org/10.1016/j.surfcoat.2018.12.003)
5. M. J. Jackson, W. Ahmed, in *Surface Engineered Surgery Tools and Medical Devices*, M. J. Jackson, W. Ahmed, Eds., Springer-Verlag, Berlin, 2007, pp. 21–47
6. C. Larsson, P. Thomsen, B.-O. Aronsson, M. Rodahl, J. Lausmaa, B. Kasemo, L. E. Ericson, *Biomaterials* **17** (1996) 605 (https://doi.org/10.1016/0142-9612(96)88711-4)
7. H. M. Kim, F. Miyaji, T. Kokubo, T. Nakamura, *J. Mater. Sci. Mater. Med.* **8** (1997) 341 (https://doi.org/10.1023/A:1018524731409)
8. T. Kokubo, H. M. Kim, M. Kawashita, T. Nakamura, *J. Mater. Sci. Mater. Med.* **15** (2004) 99 (https://doi.org/10.1023/B:JMSM.0000011809.36275.0c)
9. K. Bordji, J. Y. Jouzeau, D. Mainard, E. Payan, P. Netter, K. T. Rie, T. Stucky, M. Hage--Ali, *Biomaterials* **17** (1996) 929 (https://doi.org/10.1016/0142-9612(96)83289-3)
10. C. Sittig, M. Textor, N. D. Spencer, M. Wieland, P. H. Vallotton, *J. Mater. Sci. Mater. Med.* **10** (1999) 35 (https://doi.org/10.1023/A:1008840026907)
11. S. Stojadinović, R. Vasilić, M. Petković, B. Kasalica, I. Belča, A. Žekić, L. Zeković, *Appl. Surf. Sci.* **265** (2013) 226 (https://doi.org/10.1016/j.apsusc.2012.10.183)
12. N. Ohtsu, H. Kanno, S. Komiya, Y. Mizukoshi, N. Masahashi, *Appl. Surf. Sci.* **270** (2013) 513 (https://doi.org/10.1016/j.apsusc.2013.01.071)
13. C. Bayram, M. Demirbilek, E. Yalçin, M. Bozkurt, M. Doğan, E. B. Denkbaş, *Appl. Surf. Sci.* **288** (2014) 143 (https://doi.org/10.1016/j.apsusc.2013.09.168)
14. Y. J. Park, K. H. Shin, H. J. Song, *Appl. Surf. Sci.* **253** (2007) 6013 (https://doi.org/10.1016/j.apsusc.2006.12.112)
15. L. Xie, X. Liao, H. Xu, G. Yin, Z. Huang, Y. Yao, X. Chen, J. Gu, *Mater. Lett.* **72** (2012) 141 (https://doi.org/10.1016/j.matlet.2011.12.094)
16. D. Capek, M. P. Gigandet, M. Masmoudi, M. Wery, O. Banakh, *Surf. Coatings Technol.* **202** (2008) 1379 (https://doi.org/10.1016/j.surfcoat.2007.06.027)
17. N. Ohtsu, D. Ishikawa, S. Komiya, K. Sakamoto, *Thin Solid Films* **556** (2014) 247 (https://doi.org/10.1016/j.tsf.2014.01.083)
18. S. Komiya, K. Sakamoto, N. Ohtsu, *Appl. Surf. Sci.* **296** (2014) 163 (https://doi.org/10.1016/j.apsusc.2014.01.066)
19. X. Zhang, Y. Zhang, L. Chang, Z. Jiang, Z. Yao, X. Liu, *Mater. Chem. Phys.* **132** (2012) 909 (https://doi.org/10.1016/j.matchemphys.2011.12.032)
20. Y. Parcharoen, P. Kajitvichyanukul, S. Sirivisoot, P. Termsuksawad, *Appl. Surf. Sci.* **311** (2014) 54 (https://doi.org/10.1016/j.apsusc.2014.04.207)

21. D. F. Williams, *J. Mater. Sci.* **22** (1987) 3421 (https://doi.org/10.1007/bf01161439)
22. C. Han, Q. Wang, B. Song, W. Li, Q. Wei, S. Wen, J. Liu, Y. Shi, *J. Mech. Behav. Biomed. Mater.* **71** (2017) 85 (http://dx.doi.org/10.1016/j.jmbbm.2017.02.021)
23. K. Niespodziana, K. Jurczyk, J. Jakubowicz, M. Jurczyk, *Mater. Chem. Phys.* **123** (2010) 160 (http://dx.doi.org/10.1016/j.matchemphys.2010.03.076)
24. H. B. Wen, J. R. de Wijn, F. Z. Cui, K. de Groot, *J. Biomed. Mater. Res.* **41** (1998) 227 (https://doi.org/10.1002/(SICI)1097-4636(199808)41:2<227::AID-JBM7>3.0.CO;2-K)
25. S. A. Ulasevich, A. I. Kulak, S. K. Poznyak, S. A. Karpushenkov, A. D. Lisenkov, E. V Skorb, *RSC Adv.* **6** (2016) 62540 (https://doi.org/10.1039/C6RA10560B)
26. H. Wang, N. Eliaz, Z. Xiang, H.-P. Hsu, M. Spector, L. W. Hobbs, *Biomaterials* **27** (2006) 4192 (https://doi.org/10.1016/j.biomaterials.2006.03.034)
27. M. Geetha, A. K. Singh, R. Asokamani, A. K. Gogia, *Prog. Mater. Sci.* **54** (2009) 397 (https://doi.org/10.1016/j.pmatsci.2008.06.004)
28. J. Zhao, X. Wang, R. Chen, L. Li, *Solid State Commun.* **134** (2005) 705 (https://doi.org/10.1016/j.ssc.2005.02.028)
29. S. Eraković, A. Janković, D. Veljović, E. Palcevskis, M. Mitrić, T. Stevanović, D. Janaćković, V. Mišković-Stanković, *J. Phys. Chem., B* **117** (2013) 1633 (https://doi.org/10.1021/jp305252a)
30. Z. M. Yan, T. W. Guo, H. B. Pan, J. J. Yu, *Mater. Trans.* **43** (2002) 3142 (https://doi.org/10.2320/matertrans.43.3142)
31. K. I. Popov, P. M. Živković, N. D. Nikolić, *J. Serb. Chem. Soc.* **76** (2011) 805 (https://doi.org/10.2298/JSC100312079P)